



HAL
open science

Stability and atomic motifs of quasicrystalline models

F. Lançon, L. Billard

► **To cite this version:**

F. Lançon, L. Billard. Stability and atomic motifs of quasicrystalline models. Journal de Physique, 1990, 51 (11), pp.1099-1111. 10.1051/jphys:0199000510110109900 . jpa-00212433

HAL Id: jpa-00212433

<https://hal.science/jpa-00212433>

Submitted on 4 Feb 2008

HAL is a multi-disciplinary open access archive for the deposit and dissemination of scientific research documents, whether they are published or not. The documents may come from teaching and research institutions in France or abroad, or from public or private research centers.

L'archive ouverte pluridisciplinaire **HAL**, est destinée au dépôt et à la diffusion de documents scientifiques de niveau recherche, publiés ou non, émanant des établissements d'enseignement et de recherche français ou étrangers, des laboratoires publics ou privés.

Classification
Physics Abstracts
64.70-61.50E-02.70

Stability and atomic motifs of quasicrystalline models

F. Lançon and L. Billard

Département de Recherche Fondamentale; Service de Physique; Groupe de Métallurgie Physique;
Centre d'Etudes Nucléaires; 85X; 38041 Grenoble cedex; France

(Reçu le 8 janvier 1990, accepté le 21 février 1990)

Résumé. — Par relaxation numérique avec des potentiels inter-atomiques de paire, nous étudions la stabilité de modèles quasi-cristallins. Nous montrons qu'un modèle monoatomique et un modèle pour AlMnSi sont stables et nous présentons leurs fonctions de distributions partielles de paires. Ces structures quasi-cristallines sont décrites par des coupes tridimensionnelles de motifs atomiques eux-mêmes tridimensionnels dans un espace à six dimensions. Au cours de la relaxation, les atomes quittent leur position initiale, et nous montrons que ces déplacements correspondent à des modifications des motifs atomiques.

Abstract. — By numerical relaxation with interatomic pair potentials, we study the stability of quasicrystalline models. A monoatomic model and a AlMnSi model are found stable and we present their partial pair distribution functions. These quasicrystalline structures are described by 3D cross sections through 3D atomic motifs in a 6D space. During the relaxation, atoms move from their initial positions and we show that these displacements correspond to modifications of the atomic motifs.

1. Introduction.

Numerical studies of bidimensional quasicrystal atomic models [1-4] have led to important results about the stability of quasicrystalline structures. In particular it has been shown [3] both theoretically and numerically that a diatomic quasicrystal with a five-fold symmetry can be stable with atomic pair potentials.

Even if real atoms do not interact through pair potentials, investigation of models with simple interactions are valuable to the understanding of quasicrystals. A detailed study of the stability of quasicrystalline models has been done by Roth *et al.* [5] who found one monoatomic and one diatomic quasicrystal stable. In this paper we confirm the meta-stability of the monoatomic packing and we test a recent AlMnSi model [6] as well as different variations of it. During the simulations, the models relax to configurations which correspond to minima of the potential energy. Janssen [4] has pointed out that the displacement field should have the symmetry of the initial quasicrystalline state and, after a numerical relaxation, the final state should be a quasicrystal. Here we analyse the relaxed states within the framework of the cut-method in hyperspace [7] and we present the

modifications of the 3D atomic motifs induced by the relaxation process.

2. 3D-atomic motifs and relaxation.

2.1 6D-DESCRIPTION OF THE QUASICRYSTALS. — The four quasicrystalline models which have been relaxed can be constructed either with the strip and projection method [8,9] or with the cut-method [7]. However the last method is more general and allows a description of the final relaxed states. Let us recall the notation: let $(\epsilon_1, \dots, \epsilon_6)$ be the canonical basis of \mathbb{R}^6 . The icosahedron group leaves two 3D subspaces E^{\parallel} and E^{\perp} invariant. The space E^{\parallel} is identified with our usual physical space. Let p be the orthogonal projector onto E^{\parallel} whose kernel is the complementary space E^{\perp} , i.e. $p(E^{\parallel}) = E^{\parallel}$ and $p(E^{\perp}) = \{0\}$ and let $p' = 1 - p$. The vectors $e_i = p(\epsilon_i)$ and $e'_i = p'(\epsilon_i)$ point towards icosahedral directions in spaces E^{\parallel} and E^{\perp} respectively. The quasicrystal is the set X_t of atomic sites which are the projections onto E^{\parallel} of the intersection of the 3D space $E^{\parallel} + t$ with the 3D atomic motif A periodically set on the 6D cubic lattice \mathbb{Z}^6 (more generally there can be different atomic motifs A_i):

$$X_t = \left\{ \mathbf{x} \in E^{\parallel} \mid \mathbf{x} + \mathbf{t} = \mathbf{N} + \mathbf{a}; \begin{array}{l} \mathbf{N} \in \mathbb{Z}^6 \\ \mathbf{a} \in A \end{array} \right\} \quad (1)$$

where the vector t belongs to E^{\perp} and indices equivalent structures, and the subset A is a 3D hypersurface.

For the model before relaxation, as for any quasicrystalline structure which can also be obtained with the strip method, the atomic motifs A are 3D solids which are subsets of E^{\perp} .

2.2 NUMERICAL RELAXATION METHOD. — The total potential energy of particles which interact through a pair potential $\varphi(r)$ is

$$E_{\text{pot}} = \frac{1}{2} \sum_{i,j} \varphi(r_{ij}) \quad (2)$$

where r_{ij} is the distance between particles i and j . In the initial quasicrystal models, all site environments are inequivalent and the particles are not in stable positions. They will move to configurations where E_{pot} is a (local) minimum. This relaxation is achieved numerically [10] using the conjugate gradient method. We have used the potential $\varphi(r)$ equal to the Morse potential

$$\epsilon_0 \{ \exp[-2\alpha(r - r_0)] - 2\exp[-\alpha(r - r_0)] \}$$

for $r \leq r_1$; ϵ_0 and r_0 are, respectively, the depth and the position of the potential minimum and we have chosen α such that $\alpha r_0 = 6$. The potential $\varphi(r)$ is equal to a fifth-order polynomial between r_1 and a cut-off distance r_c , such that φ , $\partial\varphi/\partial r$ and $\partial^2\varphi/\partial r^2$ are continuous. Finally $\varphi(r) = 0$ for $r \geq r_c$.

2.3 ATOMIC SIZES. — In the monoatomic case we can set the energy and length units equal to ϵ_0 and r_0 respectively. In a diatomic structure of, say A and B particle types, there are three types of pairs: AA, AB and BB, and for each one we need the values of ϵ_0 and r_0 . The potential depths ϵ_0 are important when one deals with chemical ordering problems, but in a relaxation process very little ordering occurs and we have merely set $\epsilon_{0AA} = \epsilon_{0AB} = \epsilon_{0BB}$. On the other hand the parameters r_{0AA} , r_{0AB} and r_{0BB} define the particle "sizes" and are pertinent geometrical parameters. One could guess values for these parameters from the distances which occur, for

instance, in Al – Mn alloys. But this method is more or less arbitrary since one has the choice among different possible distances.

In their study on quasicrystal stability, Roth *et al.* [5] have optimized the potential parameters r_o by fixing the atoms at their original positions and by minimizing the potential energy with respect to r_o . Then they relaxed their stucture with these parameter values. Our method is to consider E_{pot} in equation (2) as a function of the atomic coordinates and of the parameters r_o , *i.e.*,

$$E_{pot} = f(\mathbf{x}_1, \dots, \mathbf{x}_N, r_{oAA}, r_{oAB}, r_{oBB}) \tag{3}$$

and to apply the conjugate gradient method to function f . Therefore the structure and the atomic "sizes" are relaxed simultaneously and the final values of the parameters r_o are optimized for the final structure.

2.4 PERIODIC APPROXIMANTS. — To avoid free surface effects, we use periodic approximants to quasicrystals. This can be done by giving a different orientation to the cutting space and to the physical space in the 6D space. Since we want to keep a perfect icosahedral orientational order, the physical space and the parallel space E^{\parallel} are still identified but because we need periodicity we choose a rational orientation for the cutting space E^{cut} . The periodic approximant is then the set X_t of atomic sites which are the projections onto E^{\parallel} of the intersections of $E^{cut} + t$ with the periodically repeated atomic motif A :

$$X_t = \left\{ \mathbf{x} = p(\mathbf{x}_c); \mathbf{x}_c \in E^{cut} \mid \mathbf{x}_c + t = \mathbf{N} + \mathbf{a}; \mathbf{N} \in \mathbb{Z}\mathbb{Z}^6 \right. \\ \left. \mathbf{a} \in A \right\} \tag{4}$$

where $t \in E^{\perp}$ and p is the projector previously defined.

The space E^{cut} is spanned by three vectors $(p,0,-q,0,p,q)$, $(q,p,0,-p,-q,0)$, $(0,q,p,q,0,p)$ where p and q are integers of the Fibonacci chain.

Note that in order to keep physical properties such as a prescribed minimal interatomic distance or a tiling existence, the atomic motif is slightly distorted in the periodic approximant cases. For instance to get a 3D tiling made of the Penrose rhombohedra, the atomic motif is the projection of the 6D unit cube onto E^{\perp} along E^{cut} and therefore depends on the E^{cut} orientation.

2.5 6D-DESCRIPTION OF THE RELAXED QUASICRYSTALS. — Let X_t and X_t^r be a quasicrystal before and after the relaxation. A site \mathbf{x} of X_t relaxes to a position \mathbf{x}^r . We assume that the new position \mathbf{x}^r is associated with a new atomic motif A^r located at the same point \mathbf{N} of the 6D lattice: X_t^r is defined by (1) with \mathbf{x} , \mathbf{a} and A replaced by \mathbf{x}^r , \mathbf{a}^r and A^r . It follows

$$\mathbf{x}^r - \mathbf{x} = \mathbf{a}^r - \mathbf{a} \tag{5}$$

where \mathbf{a}^r belongs to A^r . We want the values of the final motif elements \mathbf{a}^r associated with the relaxed positions \mathbf{x}^r . Since \mathbf{x} and \mathbf{x}^r belong to E^{\parallel} and \mathbf{a} belongs to E^{\perp} , equation (5) gives

$$p(\mathbf{a}^r) = \mathbf{x}^r - \mathbf{x} \quad \text{and} \quad p'(\mathbf{a}^r) = \mathbf{a} \tag{6}$$

In the periodic approximant case relation (5) is changed in $\mathbf{x}_c^r - \mathbf{x}_c = \mathbf{a}^r - \mathbf{a}$ and relations (6) becomes

$$p(\mathbf{a}^r) = \mathbf{x}^r - \mathbf{x} \quad \text{and} \quad p'(\mathbf{a}^r) = \mathbf{a} + p'(\mathbf{x}_c^r - \mathbf{x}_c) \tag{7}$$

where the corrective term $\mathbf{x}_c^r - \mathbf{x}_c$ is easily calculated from $\mathbf{x}^r - \mathbf{x}$.

Thus the new atomic motif A^r has an extent in parallel space which is directly the site displacements during the numerical relaxation. We will use equations (6) or (7) to compute the final motif elements a^r associated with the relaxed positions x^r .

The initial atomic motif A is a 3D domain included in E^\perp . It is usually represented by a projection onto a 2D sheet of paper. Actually this drawing is also a 2D representation of A^r since A is already the projection of A^r onto E^\perp (cf. relation (6)). On the other hand to see the variation between A and A^r we need to represent them in a 2D-plane which contains a direction of E^\parallel and a direction of E^\perp . We have chosen to represent sections of the atomic motifs by the planes P_5 and P_3 which are respectively the five-fold and three-fold rotation 2D-axes in 6D. Plane P_5 contains ε_6 , $\delta = \varepsilon_1 + \dots + \varepsilon_6$, $e_6 = p(\varepsilon_6)$ and $e'_6 = p'(\varepsilon_6)$. Plane P_3 contains $\varepsilon_1 - \varepsilon_2 + \varepsilon_3$ and $\varepsilon_4 + \varepsilon_5 + \varepsilon_6$. Symmetry constraints imply [7] that a^r belongs to the n -fold 2D-axis P_n when a belongs to P_n . Since simulation deals with a finite number of sites, very few elements a^r are strictly in plane P_n . Thus we consider the motif elements a^r obtained by simulation and which are in a strip of small width d around plane P_n . We plot their projections onto P_n . We have used $d = 0.2 \parallel e_i \parallel$

3. Unit-sphere packing.

The shortest distance between vertices in the standard 3D Penrose tiling is the length of the small diagonal of the oblate rhombohedron: $d_r \simeq 0.563e$ where the length unit is $e = \parallel e_i \parallel$. But only 0.76 bonds per vertex have their length equal to d_r , while the next distances are equal to e (the rhombohedron edge) and to $d_f \simeq 1.052e$ (the small diagonal of rhombohedron faces) with frequencies equal to 6 and 6.5 respectively. Henley [11] has shown that, if we suppress the d_r distances by removing as few vertices as possible (22.0%), it is possible to have a packing with spheres of diameter equal to e and with a packing fraction equal to 0.6288. Henley has called S_1 the 3D atomic motif which corresponds to such a unit-sphere packing. The volume of S_1 is directly related to the packing fraction. A precise description of S_1 has been given by Oguey and Duneau [12]: it is a stellated dodecahedron truncated by the standard triacontahedron.

We have used this atomic motif, suitably modified, to take the periodic approximation into account (see Appendix B), to build a unit-sphere packing of 8051 particles corresponding to the r -approximant $p/q = 8/5$.

Roth *et al.* [5] have shown that the unit-sphere packing is (meta-) stable when relaxed with a Lennard Jones-like pair potential. We have studied the unit-sphere packing in the case of the Morse potential and with several interaction ranges. We confirm its stability and the pair correlation functions, $g(r)$, of the relaxed states are shown in figure 1. However the relaxed state is an amorphous structure when the cut-off distance r_c of the potential φ is equal to $1.5r_0$ and $r_t = 1.15r_0$. Since the initial displacement field is supposed to have the symmetry of the initial state, we suspect that the quasiperiodic structure is slowly destroyed because of numerical rounding errors and because the initial state is an approximant of a truly quasiperiodic state. On the other hand, the quasicrystalline peaks broaden but remain when $r_c = 2r_0$ (and $r_t = 1.5r_0$). The displacement distribution $n(\parallel x^r - x \parallel)$, shown in figure 2, is very narrow with a mean displacement equal to $0.02e$ instead of $0.47e$ in the amorphous case. The optimized value of the potential minimum position is $r_0 = 1.045e$ and the potential energy per atom is equal to $-6.05\varepsilon_0$ as compared to $-6.83\varepsilon_0$ for fcc lattice and $-6.58\varepsilon_0$ for bcc lattice. The stability has also been obtained with the very short potential range $r_c = 1.2r_0$ ($r_t = 1.1r_0$), for the intermediate ranges $r_c = 1.65r_0$ ($r_t = 1.53r_0$) or $r_c = 1.8r_0$ ($r_t = 1.4r_0$), and for the long range $r_c = 3r_0$ ($r_t = 2.5r_0$).

The sections of S_1 and S_1^r by planes P_5 and P_3 are shown in figure 3. By definition S_1 is included in E^\perp while S_1^r has a small component in E^\parallel . Note that S_1^r is centrosymmetric, as can be predicted from the icosahedron symmetry of the initial state.

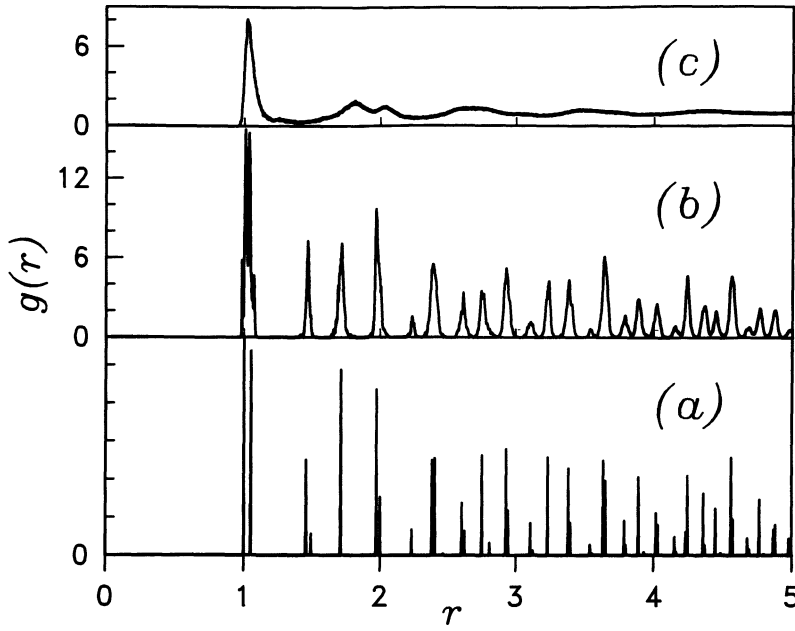


Fig. 1. — Pair correlation function $g(r)$ of the unit-sphere packing: (a) initial quasicrystal, (b) relaxed quasicrystal and (c) relaxed amorphous state. The length unit is the rhombohedron edge e .

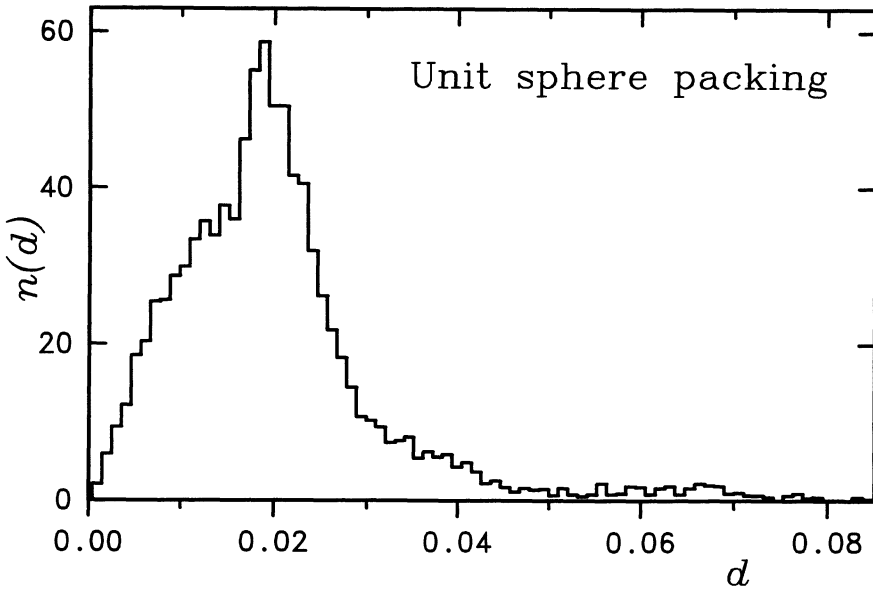


Fig. 2. — Distribution of the atomic moves $d = \| \mathbf{x}^f - \mathbf{x} \|$ between the relaxed and initial unit-sphere quasicrystals. The length unit is the rhombohedron edge e .

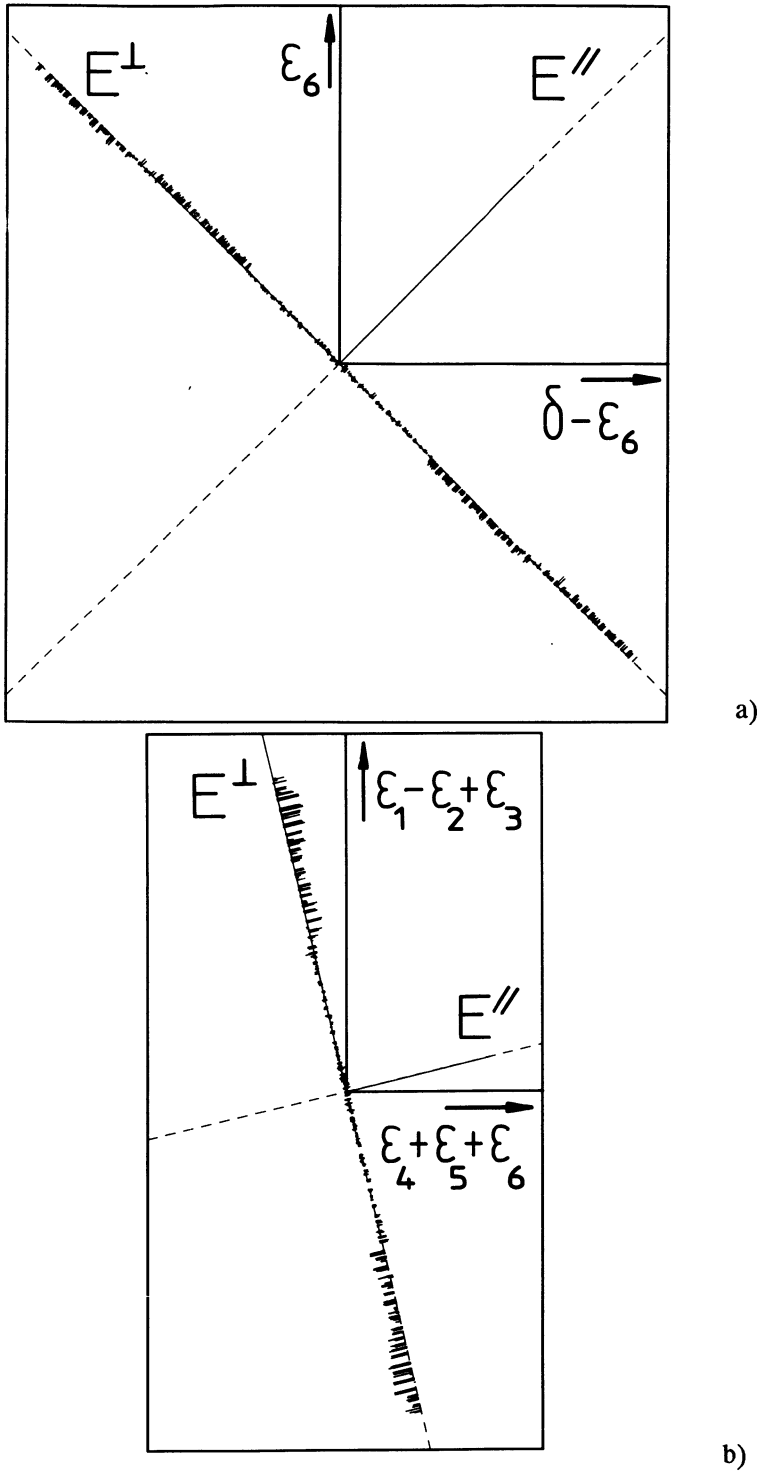


Fig. 3. — Cross section of the atomic motif corresponding to the unit-sphere packing by the symmetry planes: (a) P_5 and (b) P_3 . Segments are drawn between the initial and the final motif elements.

4. AlMnSi quasicrystal models.

4.1 THE MODEL OF DUNEAU AND OQUEY. — Duneau and Oguey [6] have proposed a model for AlMnSi icosahedral quasicrystal built upon a set of atomic motifs. The density and the concentration fit to the experimental values and the smaller interatomic distances are compatible with the distances found in corresponding crystals. The model does not distinguish between Al and Si atoms which are randomly set on the Al matrix. This model contains a large number of Mackay icosahedra [13] with no central atom.

Five atomic motifs are involved in this model. Three concentric domains are centered on the $\mathbb{Z}Z^6$ nodes : the inner domain corresponds to the central void of Mackay icosahedra, and thus this domain corresponds to vacancies; the second shell corresponds to Mn atoms and the outer domain corresponds to Al atoms. The other two atomic motifs are one dodecahedron centred at the body centers of $\mathbb{Z}Z^6$ (i.e. $\mathbb{Z}Z^6 + \delta/2$) which corresponds to Mn atoms and one solid centered at the sites $\mathbb{Z}Z^6 \pm e_i/2$, $i = 1..6$, which corresponds to Al atoms set on the inner shell of Mackay icosahedra. The sections of these atomic motifs by plane P_5 are shown in figure 7. The modifications of these atomic motifs necessary to take the periodic approximation into account are described in Appendix A.

We have relaxed a model of 10028 atoms (7940 Al and 2088 Mn) which corresponds to the τ -approximant $p/q=5/3$ and used a potential cut-off $r_c = 2r_o$ ($r_t = 1.5r_o$). A slice of the relaxed structure is shown in figure 4. The length bonds have been optimized except r_{oMnMn} because too few Mn atoms are first neighbours and the next neighbours yield too unrealistic a MnMn bond length. We have fixed $r_{oMnMn} = d_r \simeq 0.563e$ and we have obtained the optimized values $r_{oAlAl} = 0.625e$ and $r_{oAlMn} = 0.573e$. From diffraction spectra [14] one can deduce the edge length $e = 0.460\text{nm}$ and thus $r_{oAlAl} = 0.288\text{nm}$ which is very reasonable compared to the nearest neighbour distance in pure Al equal to 0.286nm .

We have checked that the numerical diffraction pattern still has sharp peaks and has kept the icosahedron symmetry. However some large atomic displacements occur during relaxation even if the overall structure remains stable. The move distribution, shown in figure 5, is broader than in the unit sphere packing case, the mean displacement being equal to $0.08e$.

The partial pair correlation functions of the relaxed model are shown in figure 6 and are in agreement with the experimental curves obtained by neutron diffraction [15]. The positions of the first peak maxima, for the model and the experiment respectively, are : 0.28nm and 0.282nm for AlAl, 0.26nm and 0.255nm for AlMn, 0.24nm and 0.267nm for MnMn.

Figure 7 shows that the relaxed atomic motifs have an extent in parallel space E^{\parallel} . Note that the motifs are periodically repeated on the 2D lattice $\mathbb{Z}Z^6 \cap P_5$ with basis vectors ε_6 and δ . The shape of the atomic sections can be understood as follows : the displacement of each atom during the relaxation, which is the parallel component of \mathbf{a} , depends on its surroundings. Now there are partitions of the atomic motif in domains which correspond to local environment classes in physical space. A given boundary corresponds to an environment change outside a given range. Two points separated by this boundary, however close they may be, generally correspond to different displacements and discontinuities of \mathbf{a}^{\parallel} generally exist on this boundary. Since thinner and thinner partitions of A can be made, two points are always on each side of a boundary. However let us consider an atomic site \mathbf{x} corresponding to the atomic motif element \mathbf{a} ; atomic sites corresponding to motif elements closer and closer to \mathbf{a} have a larger and larger domain around them with the same environment as around \mathbf{x} and thus the displacement of these sites is more and more similar more similar to that of \mathbf{x} . Therefore the discrete points obtained by the simulation lie on a discontinuous curve but with discontinuities which are small except on the boundary locations of coarse partitions of the atomic motif.

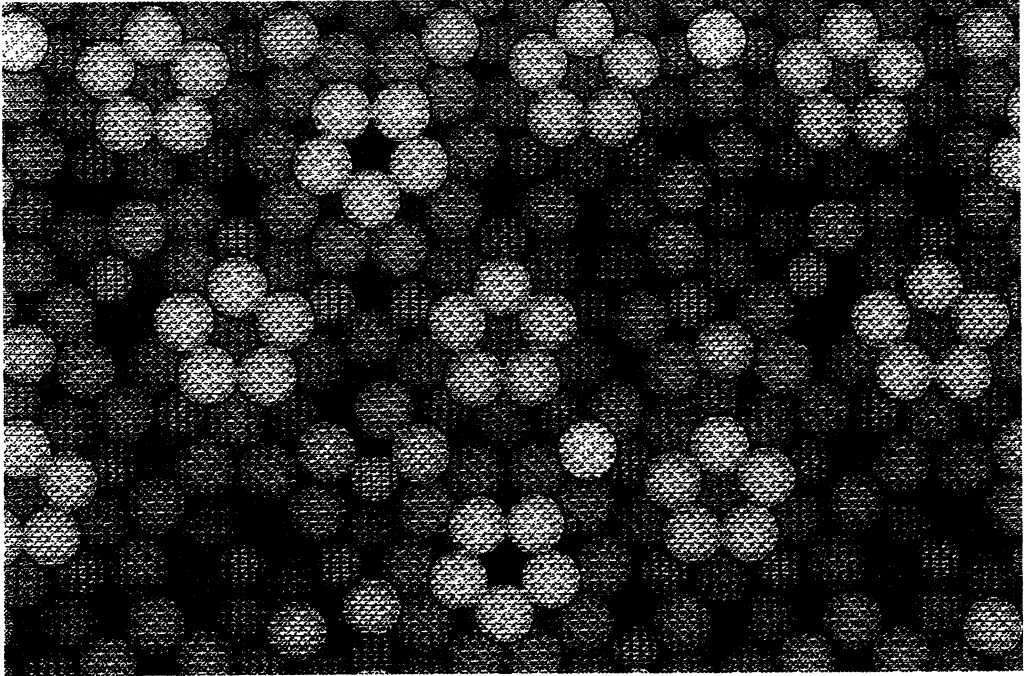


Fig. 4. — View of the relaxed AlMnSi model. Al atoms are represented by large spheres and Mn atoms by small ones. The depth is indicated by darkness.

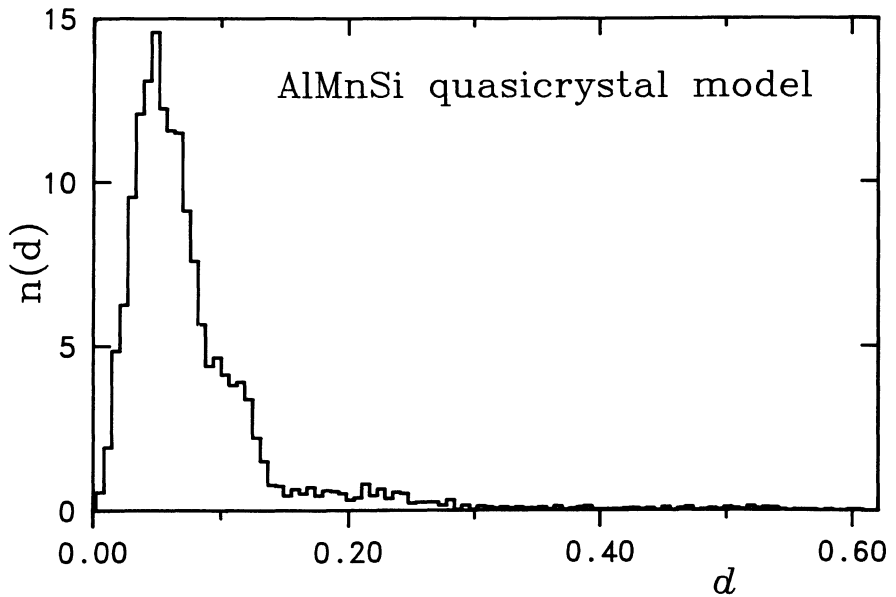


Fig. 5. — Distribution of the atomic moves $d = \| \mathbf{x}^r - \mathbf{x} \|$ between the relaxed and initial AlMnSi quasicrystals. The length unit is the rhombohedron edge e .

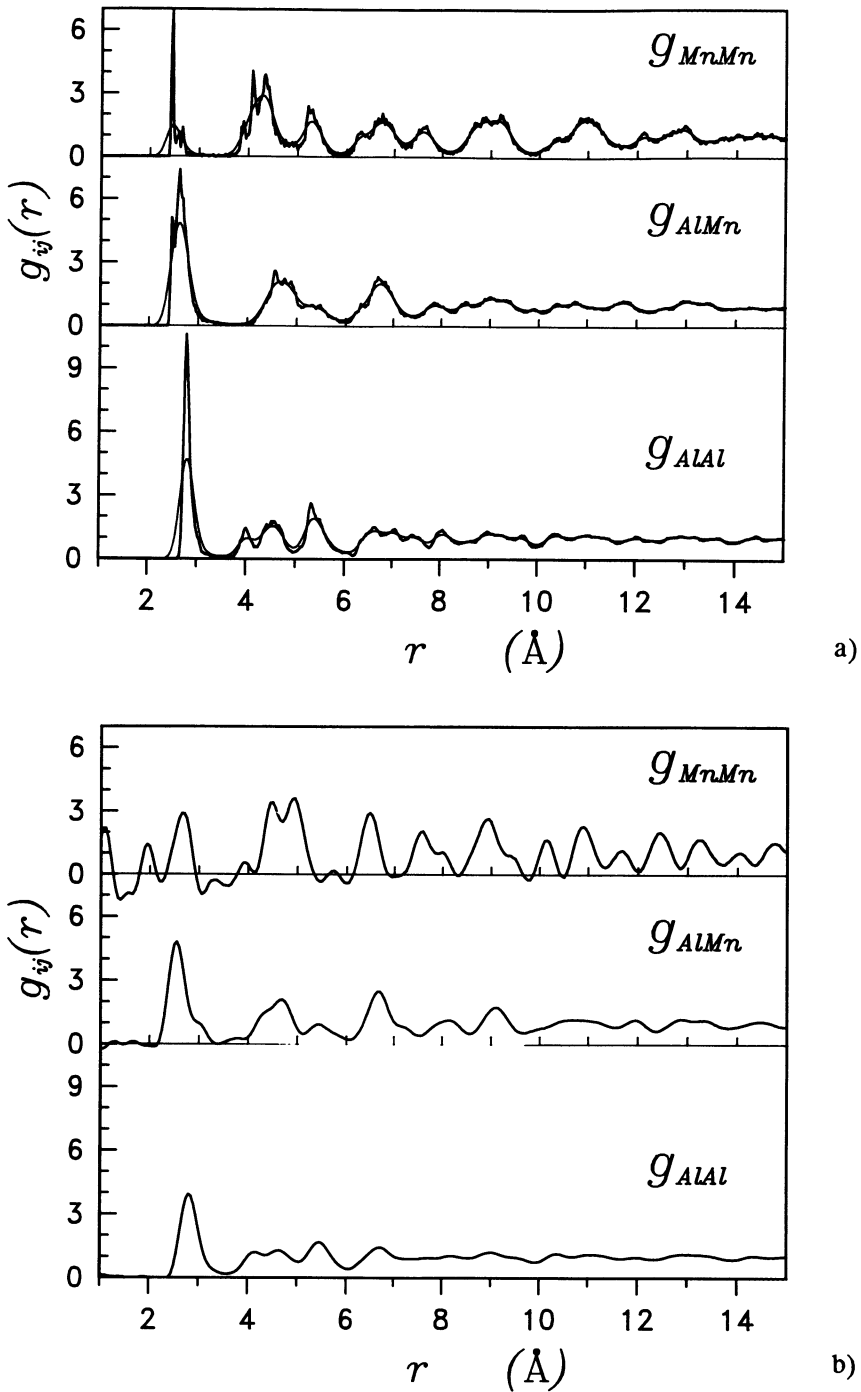


Fig. 6. — Partial pair correlation functions $g_{ij}(r)$ of $AlMnSi$ quasicrystal. (a) relaxed model curves represented as a thick line; the thin line has been obtained with a Debye-Waller factor to take into account thermal vibrations with a root mean-square displacement equal to 0.15\AA . (b) experimental curves [15].

4.2 VARIATION OF THE $AlMnSi$ QUASICRYSTAL MODEL. — We have studied two models which are simple variations of the model of Duneau and Oguey.

The first model has been considered because one cannot rule out the possibility of an occupancy of the central site of a Mackay icosahedron. Moreover, the distance between the central site and the Al neighbours is equal to the nearest neighbour distance Mn – Al and in the relaxed model the central void is even larger. Therefore we have set a Mn atom on the central site of a Mackay icosahedron, i.e., the inner domain is a Mn atomic motif. We have built a model with 10152 atoms (7940 Al and 2212 Mn).

In the second model we have taken into account the experimental results of Janot *et al.* [16] which have found one central Mn atomic motif, surrounded by an Al shell and one Al domain set on body center positions. These results suggest to associate Mn atoms with the central domain as in the previous model and to associate Al atoms instead of Mn atoms with the body center domain. Except for these modifications, we have kept the Duneau and Oguey domain shapes and volumes, which are not exactly those of Janot *et al.*, thus leading to a model of 10152 atoms (8076 Al and 2076 Mn).

The relaxation of both models produces similar results: the structures remain stable, the atomic displacements have the same average values as in the model of Duneau and Oguey, the partial pair correlation functions are only slightly different. The main differences are summarized in table I where the numbers of nearest neighbours are presented.

Table I. — Numbers of neighbours of each type, up to 0.32nm or 0.36nm, and Mn atomic fraction x_{Mn} in the relaxed $AlMnSi$ models described in the text: (a) model of Duneau and Oguey; (b) first variation; (c) second variation.

	AlAl	AlMn	MnAl	MnMn	X_{Mn}
	0.32nm – 0.36nm	0.32nm – 0.36nm	0.32nm – 0.36nm	0.32nm – 0.36nm	
(a)	9.1 – 9.5	2.7 – 2.8	10.2 – 10.6	0.7 – 0.7	0.209
(b)	9.2 – 9.6	2.9 – 3.0	10.3 – 10.7	0.6 – 0.6	0.218
(c)	9.3 – 9.7	2.7 – 2.8	10.06 – 11.0	0.2 – 0.3	0.205

5. Conclusion.

We have carried out numerical simulations of quasicrystal models by building periodic approximants and using numerical relaxation with a Morse potential. The first one is a dense monoatomic packing introduced by Henley [11] and already studied by Roth *et al.* [5]. During relaxation the atomic moves are small and the final state is metastable. The second one is a $AlMnSi$ model introduced by Duneau and Oguey [6]. Although it is stable, large atomic moves occur during relaxation. The pair correlation functions computed on the final state agree with the experimental results. Two variants of this model have also been studied and give similar results.

For both models, the relaxed state has been described in the 6D-crystallography framework where atoms are viewed as three-dimensional motifs. In the initial states these 3D motifs are usual solids, while in the relaxed states they have components in the physical space.

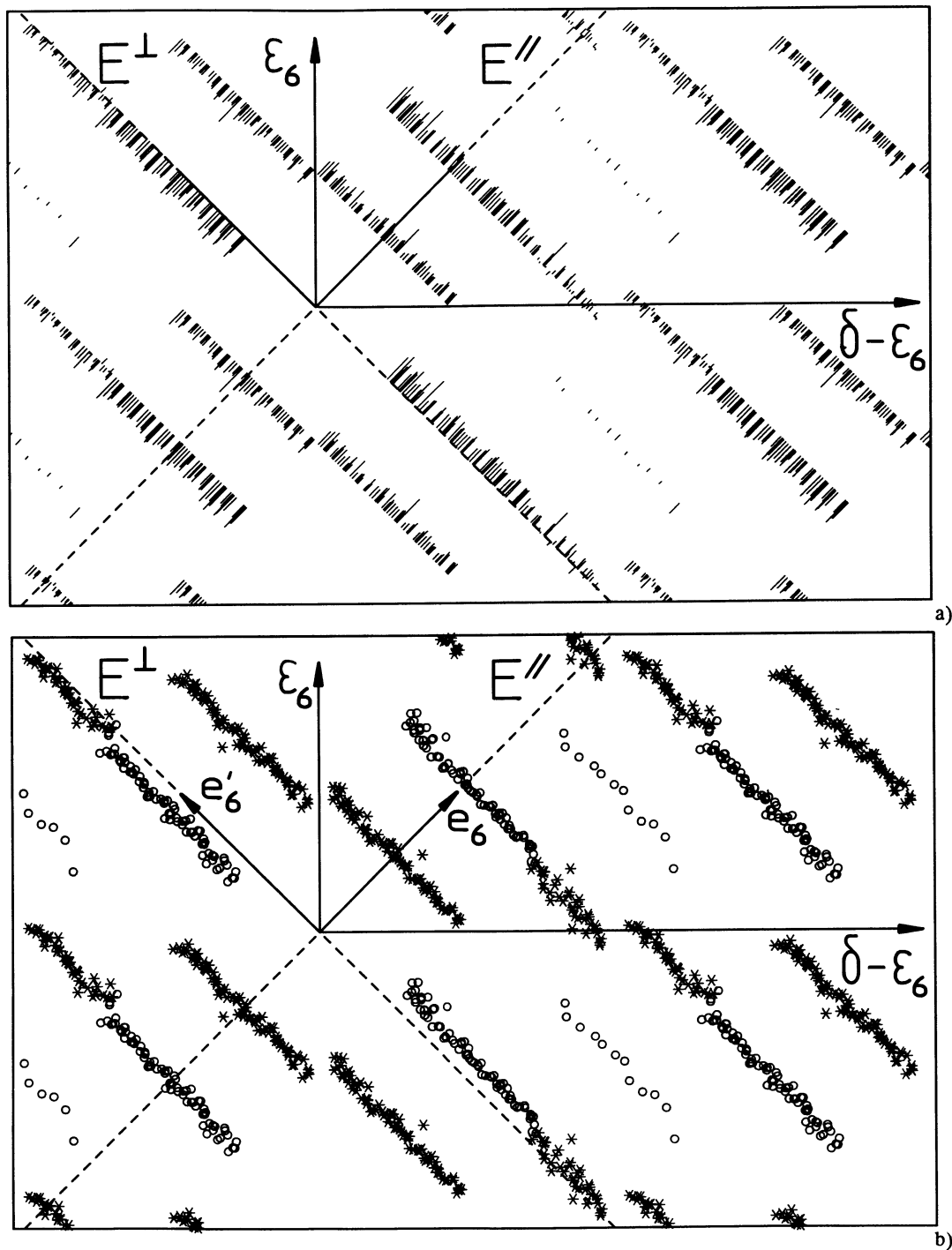


Fig. 7. — Cross section of the periodically repeated AlMnSi atomic motifs by the symmetry plane P_5 . (a) segments are drawn between the initial and the final motif elements. (b) final motifs only where Al elements are represented by circles and Mn elements by crosses.

Acknowledgements.

We thank Dr Marc de Boissieu for having sent us the experimental data of figure 6.

Appendix A

ATOMIC MOTIFS OF THE AlMnSi MODEL. — The atomic motifs proposed by Duneau and Oguey [6] were designed to imply physical properties such as a minimum interatomic distance. To conserve these properties in periodic approximants, the atomic motifs should be slightly modified.

To forbid interatomic distances lower than r_{\min} , one selects points in $\mathbb{Z}\mathbb{Z}^6$ with an auxiliary strip which is a cylinder along E^\perp with a spherical basis of radius r_{\min} in E^\parallel [12]. We project these points along the cutting space E^{cut} onto E^\perp ; the atomic motif is the Voronoï cell, around the origin, of these projected points. In the limiting case of the quasicrystal, E^{cut} is equal to E^\parallel and the atomic motifs are the polyhedra described in [6].

To obtain the 3D Penrose tiling approximants, we project the 6D unit-cube in the same way as above. Then the atomic motif is a slightly distorted triacontahedron.

In the construction of Duneau and Oguey [6] small parts of these atomic motifs are removed to forbid some atomic configurations. In our simulations these configurations have been excluded directly in the physical space E^\parallel .

Appendix B

ATOMIC MOTIF OF THE UNIT SPHERE PACKING. — A description of the atomic motif which corresponds to the quasicrystalline unit sphere packing has been given by Oguey and Duneau [12]. It is the intersection of two polyhedra: the first is the triacontahedron which selects the 3D Penrose lattice sites; the second polyhedron is a stellated dodecahedron which cannot contain the vector $\mathbf{f} = \mathbf{e}'_1 + \mathbf{e}'_3 - \mathbf{e}'_6$ and those obtained by applying the icosahedral symmetry and thus forbids the small diagonal distance $d_r = \|\mathbf{e}_1 + \mathbf{e}_3 - \mathbf{e}_6\|$. This solid is not convex and is larger than the Voronoï polyhedron which excludes the distance $r_{\min} = d_r$ (see Appendix A). To determine how the stellated dodecahedron is distorted in the periodic approximant case, we describe it in a way which generalizes the Voronoï construction.

We want a domain D of E^\perp which does not contain a vector \mathbf{f} , i.e., $\forall M$ and $N \in D$, $MN \neq \mathbf{f}$. Let $\mathbf{v}_1, \mathbf{v}_2$ and \mathbf{v}_3 be three vectors of E^\perp such that \mathbf{f} does not belong to the planes defined by two of them. Let D_1 be the domain bounded by two parallel planes:

$$D_1 = \{\lambda \mathbf{v}_2 + \mu \mathbf{v}_3 + \nu \mathbf{f} / (\lambda, \mu) \in \mathbb{R}^2, \nu \in]-1/2, 1/2[\}$$

Domains D_2 and D_3 are defined in the same way. This definition implies: $M \in D_1 \Rightarrow M + \mathbf{f} \notin D_1$ which is also true for the domain $D = (D_1 \cap D_2) \cup (D_2 \cap D_3) \cup (D_3 \cap D_1)$.

For the forbidden vector $\mathbf{f} = \mathbf{e}'_1 + \mathbf{e}'_3 - \mathbf{e}'_6$ in the quasicrystalline unit sphere packing, we take $\mathbf{v}_1 = \mathbf{e}'_5 - \mathbf{e}'_1$, $\mathbf{v}_2 = \mathbf{e}'_6 - \mathbf{e}'_2$ and $\mathbf{v}_3 = \mathbf{e}'_4 - \mathbf{e}'_3$ which define a domain D . The stellated dodecahedron is the intersection of the ten domains deduced from D by the icosahedron symmetry.

In the approximant case, the atomic motif should not contain the vectors \mathbf{f} which are the projections of $\varepsilon_1 + \varepsilon_3 - \varepsilon_6$, and the symmetrical vectors, along E^{cut} onto E^\perp . Therefore the atomic motif is defined as above with the \mathbf{e}'_i , which are the projections of ε_i along E^\parallel onto E^\perp , replaced by the projections of ε_i along E^{cut} onto E^\perp .

References

- [1] LANÇON F. and BILLARD L., *Europhys. Lett.* **2** (1986) 625-629.
- [2] WIDOM M., STRANDBURG K.J., SWENDSEN R.H., *Phys. Rev. Lett.* **58** (1987) 706-709.
- [3] LANÇON F. and BILLARD L., *J. Phys. France* **49** (1988) 249-256.
- [4] JANSSEN T., in *Quasicrystalline Materials* (cf. Ref. [17]) (1988) 327-336.
- [5] ROTH J., BOHSUNG J., SCHILLING R. and TREBIN H.-R., in *Quasicrystalline Materials* (cf. Ref. [17]) (1988) 65-74.
- [6] DUNEAU M. and OGUEY C., *J. Phys. France* **50** (1989) 135-146.
- [7] BAK P., *Phys. Rev. Lett.* **56** (1986) 861-864.
- [8] DUNEAU M. and KATZ A., *Phys. Rev. Lett.* **54** (1985) 2688-2691.
- [9] ELSENER V., *Phys. Rev. B* **32** (1985) 4892-4898.
- [10] LANÇON F., BILLARD L. and CHAMBEROD A., *J. Phys. F:Met. Phys.* **14** (1984) 579-591.
- [11] HENLEY C.L., *Phys. Rev. B* **34** (1986) 797-816.
- [12] OGUEY C. and DUNEAU M., *Europhys. Lett.* **1** (1988) 49-54.
- [13] MACKAY A.L., *Acta Cryst.* **15** (1962) 916-918.
- [14] PORTIER R., SHECHTMAN D., CAHN J. and GRATIAS D., *J. Microsc. Spectrosc. Electron.* **10** (1985) 107.
- [15] DUBOIS J.M., JANOT C. and de BOISSIEU M., in *Quasicrystalline Materials* (cf. Ref. [17]) (1988) 97-106.
- [16] JANOT C., de BOISSIEU M., DUBOIS J.M. and PANNETIER J., *J. Phys.: Condensed Matter* **1** (1989) 1029-1048.
- [17] *Quasicrystalline Materials* (Proc. of the ILL/CODEST workshop, 1988) C. Janot and J.M. Dubois Eds (World Scientific, Singapore).